



AEE 461 Design of Aircraft Structures

Lecturer: Murat ÇELİK

Lecture #7

Axial and Bending Members – cont'd

Solution:

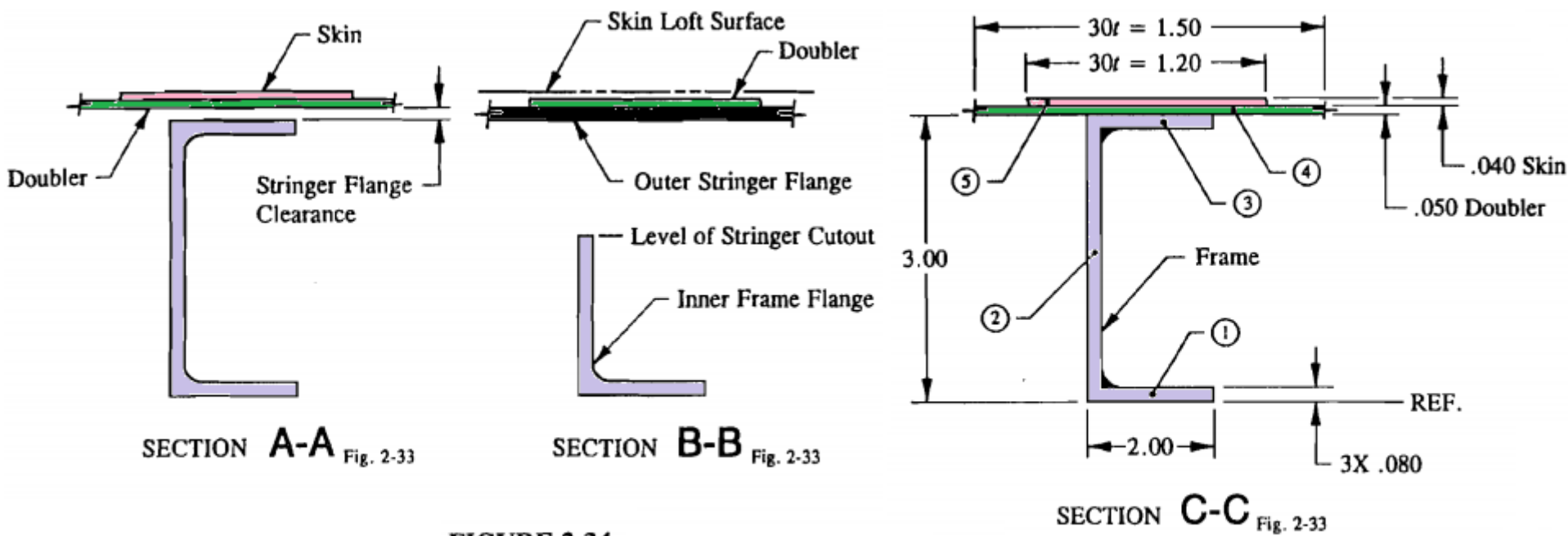


FIGURE 2-34
FIGURE 2-35
Fuselage frame cross-sectional areas.

Solution – cont'd:

The following steps have been collectively accumulated and should now be reviewed in advance of performing the actual stress analysis:

- 1) The basic frame structure is analyzed by conventional stress analysis methods at Sections A-A and B-B, Fig. 2-34, for the combined effects of axial and bending stresses at the extreme fibers. The stress values are then compared to the prescribed mechanical properties of the material and in some cases to more stringent design limitations or requirements that may have been imposed on the structure for fuselage frame design, such as inter-rivet buckling, crippling, fatigue, deformations, etc. Use only those structural members of a section area which can most efficiently carry the primary design loads of the basic frame structure.

Solution – cont'd:

- 2) After the frame structure is sized and is found to be of adequate structural strength, use Section C-C, Fig. 2-35, as a basis for a typical frame section and find the internal member forces of designated element areas of that section area. To approximate the amount of effective width of aluminum skin and doubler in compression use $30t$ (30 times the individual material thickness t).
- 3) Indicate the structural members that can provide the most direct load paths for the internal member forces of discontinuous members across the joint. Then, transfer these forces across the joint through the end fasteners of these structural members.
- 4) To complete the analysis, the shear forces and stresses across the joint are combined with the longitudinal shear forces and stresses of the main fuselage shell, respectively. The transfer of shear forces in both circumferential and longitudinal directions are algebraically combined into a single resultant shear force using Eq. A-6 of Appendix A.

Solution – cont'd:

In the vicinity of the stringer cutout, Section C-C is taken as the most representative cross-section of frame structure, where the local discontinuities and member irregularities of the joint have been avoided. In fact, even the filler material (see Fig. 2-33) is omitted from the section properties. Using the tabulation method of Appendix F, the following table is set up to compute the section properties of Section C-C:

Element	b	h	y	A	Ay	Ay^2	I_o
1	2.000	0.080	0.040	0.160	0.006	0.000	0.000
2	0.080	2.840	1.500	0.227	0.341	0.511	0.153
3	2.000	0.080	2.960	0.160	0.474	1.402	0.000
4	1.500	0.050	3.025	0.075	0.227	0.686	0.000
5	1.200	0.040	3.070	0.048	0.147	0.452	0.000
Total				0.670	1.195	3.051	0.153

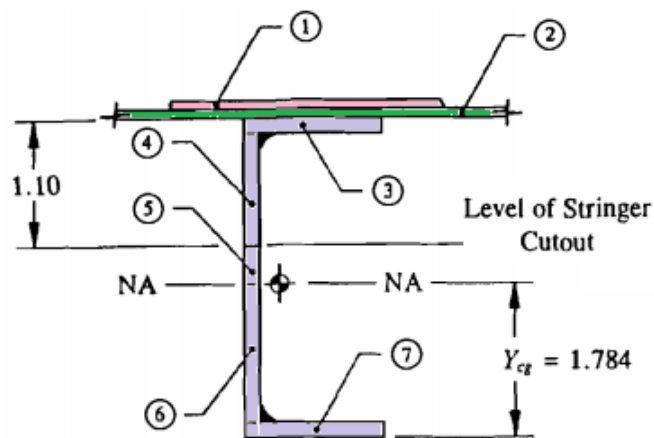
$$Y_{cg} = \frac{\sum Ay}{\sum A} = \frac{1.195}{.670} = 1.784 \text{ in}$$

$$I_{cg} = \sum I_o + \sum Ay^2 - Y_{cg}(\sum Ay)$$

$$I_{cg} = .153 + 3.051 - 1.784(1.195) = 1.072 \text{ in}^4.$$

Solution – cont'd:

With all of the section properties known, the axial and bending elastic stress distributions which are represented across the frame area in Fig. 2-33 can now be replaced by equivalent internal forces designated at specific element areas.



Elem.	Member	b	h	A	c	f_n	f_b	f^*	p^\dagger
1	skin	1.200	0.040	0.048	1.286	- 2,985	- 4,799	- 7,784	- 374
2	doubler	1.500	0.050	0.075	1.241	- 2,985	- 4,631	- 7,616	- 571
3	outer frame flange	2.000	0.080	0.160	1.176	- 2,985	- 4,388	- 7,373	- 1,180
4	portion of web (cutout)	0.080	1.020	0.082	0.626	- 2,985	- 2,336	- 5,321	- 436
5	web above the neutral axis	0.080	0.116	0.009	0.058	- 2,985	- 216	- 3,201	- 29
6	web below the neutral axis	0.080	1.704	0.136	0.852	- 2,985	3,179	194	26
7	inner frame flange	2.000	0.080	0.160	1.744	- 2,985	6,507	3,522	564

* $f = f_n + f_b$ where: $f_n = \pm P/A$ (see Eq. 2-2)
 $f_b = \pm Mc/I_{na}$ (see Eq. 2-5).

† $p = fA$ (see Eq. 2-10).

Solution – cont'd:

To help illustrate the transfer of forces across the stringer cutout, all internal member forces are conveniently drawn at the centroids of their corresponding element areas, as shown in Fig. 2-37. From our previous discussions of splice-joint analysis, it is observed here that the skin, web, and outer frame flange members that were cut away will transfer their internal member forces through each of the two end fasteners of the stringer flange. The doubler in this case will provide a continuous load path across the joint. As such, this member will not transfer its internal force to other adjacent structural members. Instead, it will be a recipient of the internal skin forces.

It is conservatively assumed here that all of the internal member force that is carried by the cut web (element #4) will transfer through the two end fasteners of the stringer flange. The reason that this is so, is that since fuselage design stresses are normally kept relatively low, most of the load carried by this member will likely transfer through the end fasteners of the stringer flange. Moreover, after all joint frictional effects have been overcome, it is generally accepted engineering practice to equally divide

Solution – cont'd:

the total member force between end fasteners of equal strength (see multi-riveted connection analysis in Chapter 3). This is shown in Fig. 2-38 for each of the two fasteners of the stringer flange. In the final step, the shear transfer forces of each fastener are logically reasoned out and their values described diagrammatically in this figure. Although many other variations of a stringer cutout are physically possible, the approaches and techniques to their analyses remain very similar.

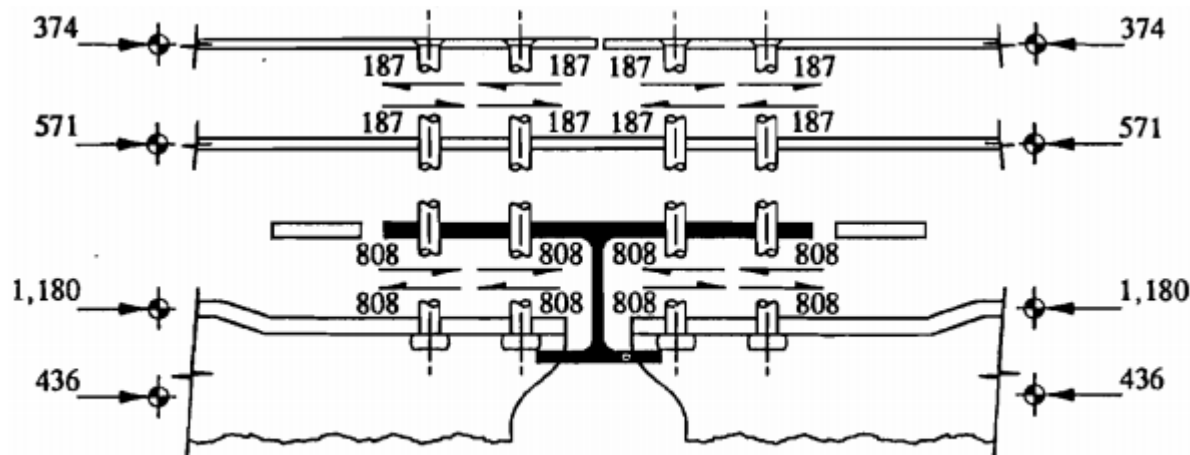


FIGURE 2-38 Transfer of shear through the end fasteners of the stringer cutout.

Rivet force transferred to stringer flange from skin and doubler:

$$374/2 = 187 \text{ lb};$$

Rivet force transferred to stringer flange from frame:

$$1180 + 436 = 1616$$

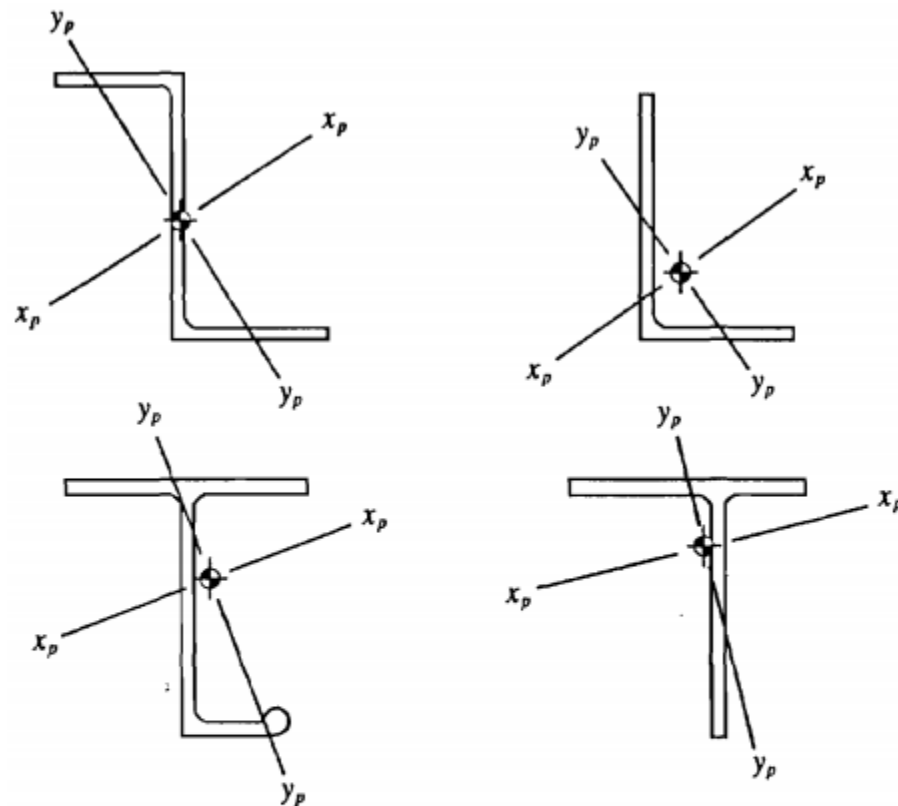
$$1616/2 = 808 \text{ lb.}$$

It is excluded from this course topics!!!

It is excluded from this course topics!!!

The limitations imposed thus far in the preceding sections of this book have been restricted to beam cross-sectional areas with at least one axis of symmetry (see complete details in Sec. 2.3, "Bending of Beams in One Plane"). While these limitations have been useful in the elementary discussions of bending fundamentals up to now, they are too restrictive and impractical to use in a wider range of beam design selections that are available for general aircraft usage. In order to expand on the concepts and principles of compound bending (beams that bend in two planes), these restrictions will be completely relaxed. The beam structure that will be illustrated in the example problem in this section will consider the more general case of a cross-sectional area having no definite axes of symmetry. Several cross-sectional areas that fit this general category are presented in Fig. 2-49.

2.9 Complex Bending Stresses of Beams



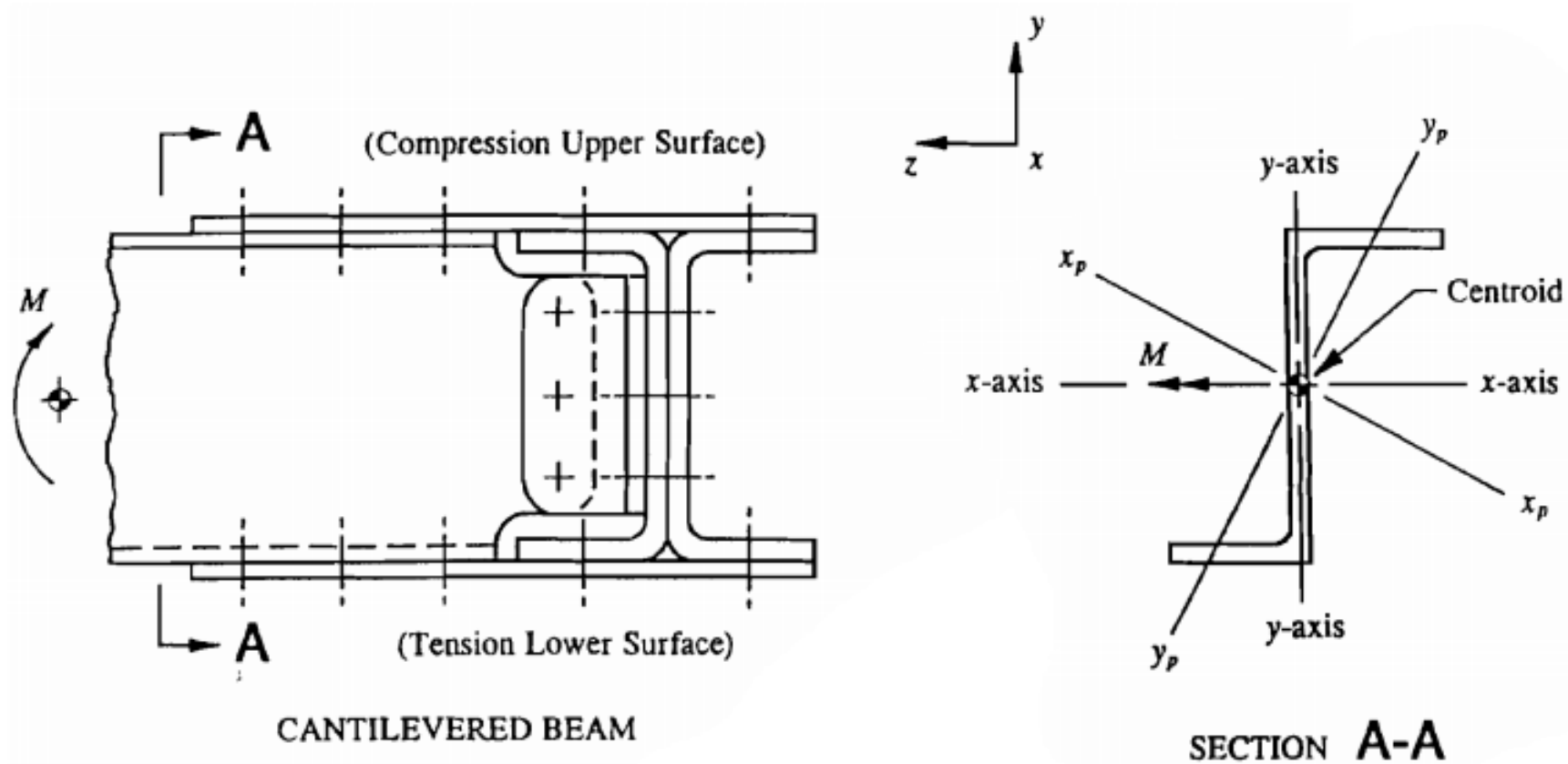
x_p = maximum principal moment of inertia
 y_p = minimum principal moment of inertia
 \diamond = centroid of area (or geometric center)

FIGURE 2-49 Principal bending axes of beam sections having no definite axes of symmetry.

2.9 Complex Bending Stresses of Beams

It will therefore be the main emphasis of this section to determine the bending stresses that develop when beams having such cross-sectional areas are subjected to bending moments which do not lie in the planes of either of the principal bending axes. The method of solution is rather straightforward, each bending moment is resolved into components that act in planes which contain the principal bending axes of the cross-sectional area. In this way, the well-known flexure formula ($f_b = \pm Mc/I_{na}$) as it applies to elastic stress design of beams can be fully utilized as a separate problem around each axis of bending. To illustrate this type of compound or multi-bending system, the cantilevered beam structure depicted in Fig. 2-50 is used. Note particularly that the cross-sectional area of the beam (Section A-A in this figure) does not have an axis of symmetry. Nor does the applied bending moment M lie in planes coincident with the principal bending axes of the section. Instead, the bending moment is applied around the horizontal x -axis of the beam.

2.9 Complex Bending Stresses of Beams



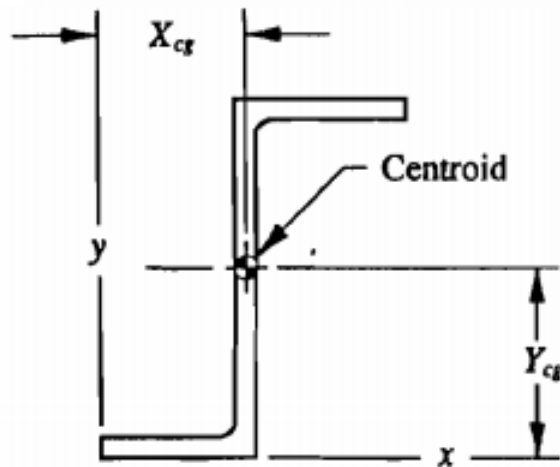
x -axis = horizontal axis about which the bending moment M is applied.

FIGURE 2-50 Section area of a cantilevered beam showing its principal axes of bending.

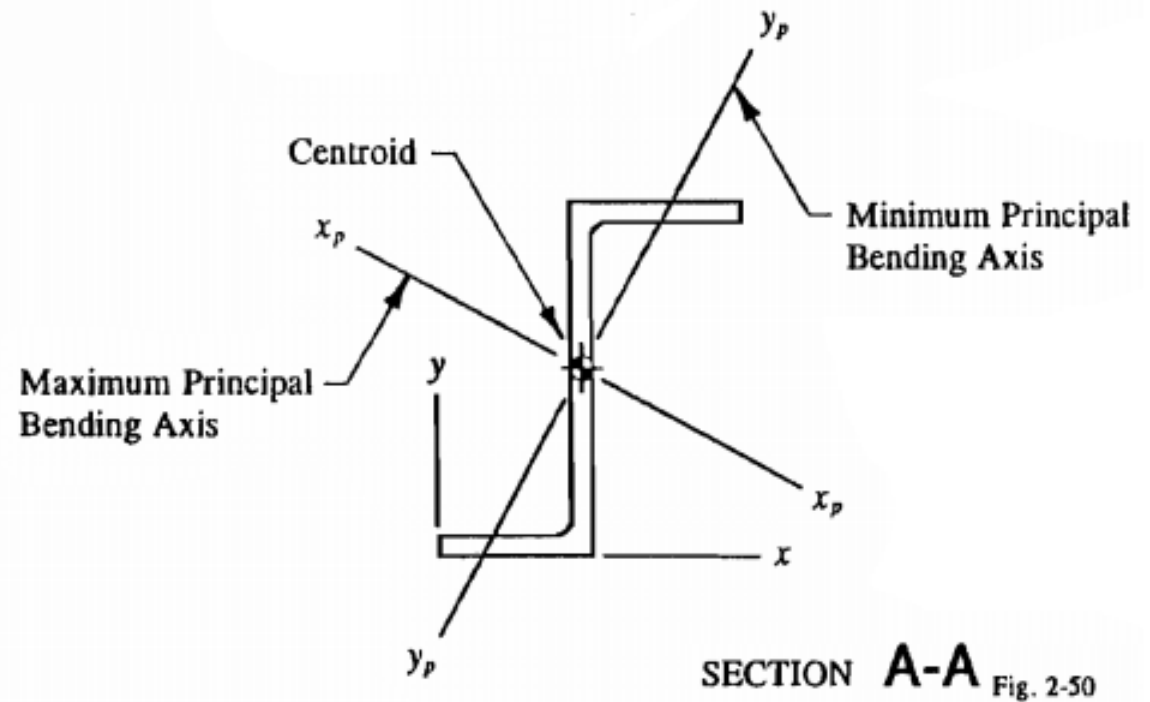
2.9 Complex Bending Stresses of Beams

To establish the true internal state of stress that will develop for such a member, the following step-by-step procedure is proposed and summarized below:

- 1) Locate the center of gravity (centroid) of the cross-sectional area around an arbitrary chosen set of horizontal and vertical reference axes x and y , as shown in Fig. 2-51. This is most easily done using Eq. A-10 of Appendix F ($Y_{cg} = \Sigma Ay / \Sigma A$).
- 2) Locate the principal bending axes x_p and y_p through the centroid of the cross-sectional area. Then calculate the principal moments of inertia I_{x_p} and I_{y_p} around these axes (see Appendix G, "Calculation of Principal Moments of Inertia," for explicit details of these computations). The principal bending axes are shown in Fig. 2-52.



SECTION A-A Fig. 2-50



SECTION A-A Fig. 2-50

FIGURE 2-51 Cross-sectional area of a beam showing the location of the centroid.

FIGURE 2-52 Cross-sectional area of a beam showing its principal axes of bending.

- 3) Resolve the applied bending moment M into equivalent component moments, $M_{x_p} = M \cos \beta$ and $M_{y_p} = M \sin \beta$, in planes coincident with the principal bending axes that pass through the centroid of area of the section. This can be viewed in Fig. 2-53, where the resolution of this bending moment is done in the same way as when a force is resolved into an equivalent system of component forces (Eqs. A-4 and A-5 in Appendix A, "Resolution of Forces," are used for this computation).
- 4) In Fig. 2-54, the bending stress distributions across the entire section area for each component of bending are computed around the principal bending axes x_p and y_p using the flexure formula ($f_b = \pm Mc/I_{na}$) developed in Sec. 2.3. Each separate stress calculation is then algebraically combined using the Principle of Superposition' as it relates to the design of elastic structural members.

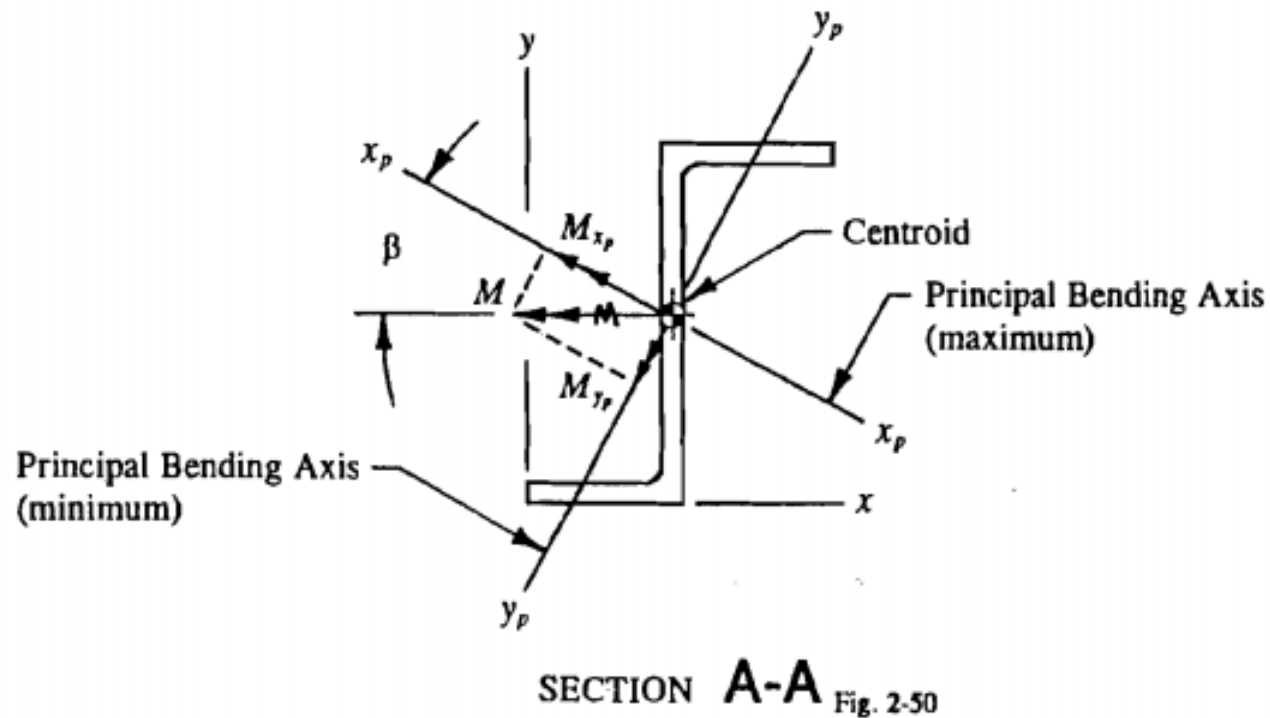


FIGURE 2-53 The moment M resolved into equivalent component moments acting in planes containing the principal bending axes.

2.9 Complex Bending Stresses of Beams

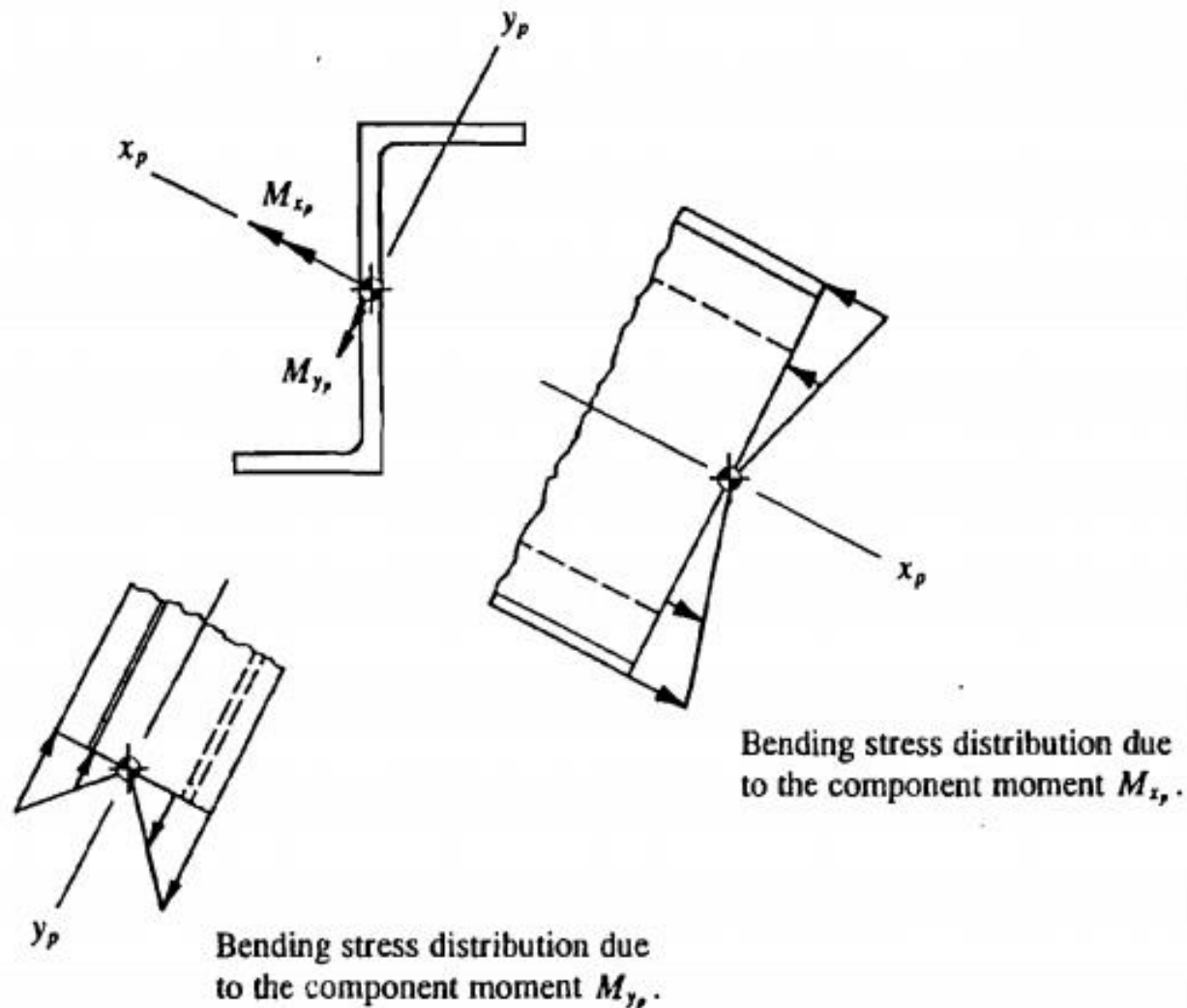


FIGURE 2-54 Bending stress distributions for the equivalent component moments.

2.9 Complex Bending Stresses of Beams

Thus, the following general expression is written for a compound bending system described in two different planes of bending:

$$f_b = \pm \frac{M_{x_p} c_{y_p}}{I_{x_p}} \pm \frac{M_{y_p} c_{x_p}}{I_{y_p}}$$

where: M_{x_p} and M_{y_p} = bending moments around the principal bending axes x_p and y_p , respectively,
 c_{x_p} and c_{y_p} = distances measured perpendicular from the principal bending axes x_p and y_p , respectively, to any point on the cross-sectional area being examined,
 I_{x_p} and I_{y_p} = moment of inertia around the principal bending axes x_p and y_p , respectively, passing through the centroid of area of the cross-sectional area.

If there is normal force, additionally, then following expression can be written as

$$f = \pm \frac{P}{A} \pm \frac{M_{x_p} c_{y_p}}{I_{x_p}} \pm \frac{M_{y_p} c_{x_p}}{I_{y_p}}$$

Example 2-6:

Consider the homogeneous beam structure in Fig. 2-56 in which an axial tension force of 2,500 lb is applied through the lower flanges of the beam. For this eccentrically loaded member, determine the critical combinations of tension and compression stresses as computed by Eq. 2-21.

Note that; the rectangular coordinate system adopted for this beam is based on the principles of right-hand rule. Using these principles, the indicated direction of the x-axis can be properly designated by the index finger of the right-hand which goes into the plane of this page. And it is further assumed that stability and buckling are not primary influences in the overall design integrity of this member. Therefore, the member is not to be considered a beam-column, at least for this analysis.

Example 2-6 cont'd:

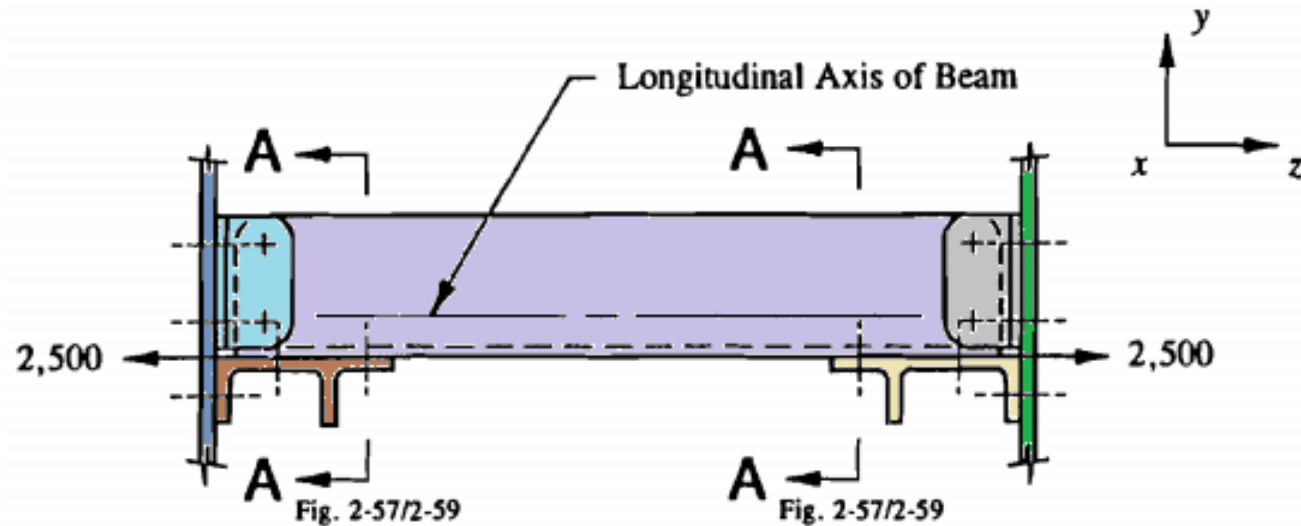


FIGURE 2-56 Eccentrically loaded beam. Axial tension force applied through the lower flanges of the beam.

Solution :

Since the axial tension force is not applied in line with the centroidal axis of the beam structure, an offset or eccentricity of load e will develop. The eccentricity is viewed on the surface of the cross-sectional area in Fig. 2-57.

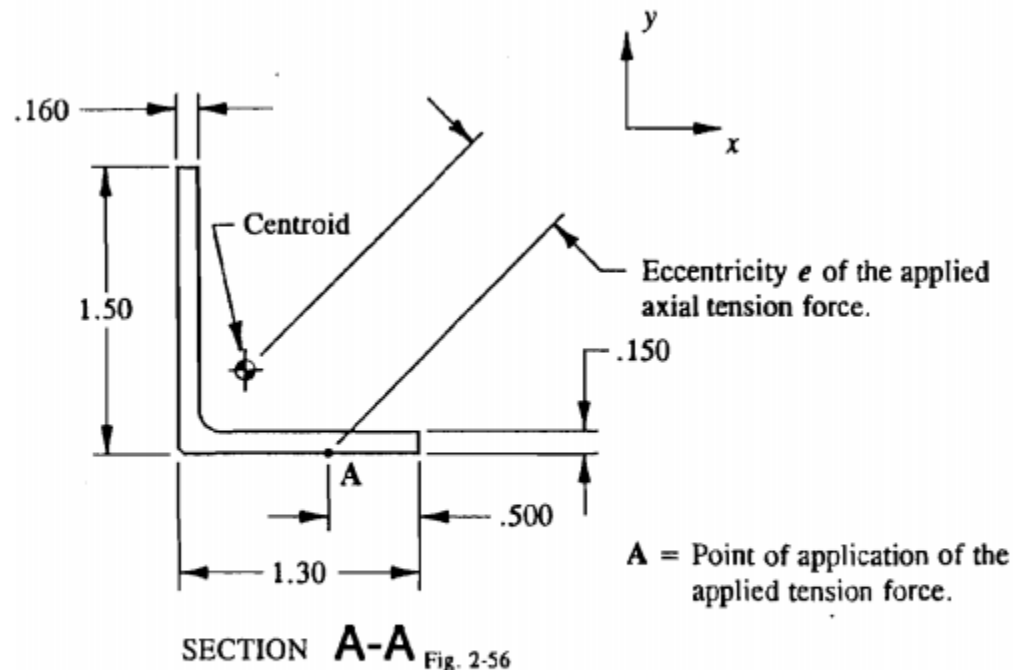


FIGURE 2-57 Eccentricity measured from the centroid of the cross-sectional area to the point of application of the applied tension force.

Solution – cont'd:

Its numerical value is measured from the centroid of the cross-sectional area to the point of application of the applied tension force. Only after the location of the centroid of area of the beam has been precisely defined can the magnitude of this eccentricity be accurately measured. Until then, all computations will be performed in terms of this unknown value.

The usual conventional methods of internal loads analysis are employed in the solution of this example problem. A section cut is passed through the cross-sectional area of the beam at Section A-A (Fig. 2-56) perpendicular to the longitudinal axis of the member. The isolated beam segments to either side of the section cut are then separated and the internal forces V , P , and M required to establish equilibrium are determined. This is shown in Fig. 2-58. For this example, the left-hand segment is chosen for the actual computation of these quantities. The proper orientation of these same loads on the right-hand segment will follow directly from the basic definitions of compatibility of internal loads at this section.

Solution – cont'd:

Now, utilizing the equations of static equilibrium, the internal forces necessary to balance the left-hand segment of this beam are computed:

$$\Sigma F_y = 0, \quad V = 0$$

$$\Sigma F_z = 0, \quad -2500 + P = 0, \quad P = 2500 \text{ lb}$$

$$\Sigma M_{cg} = 0, \quad +\curvearrowright 2500(e) - M = 0, \quad M = 2500(e) \text{ in-lb}^2.$$

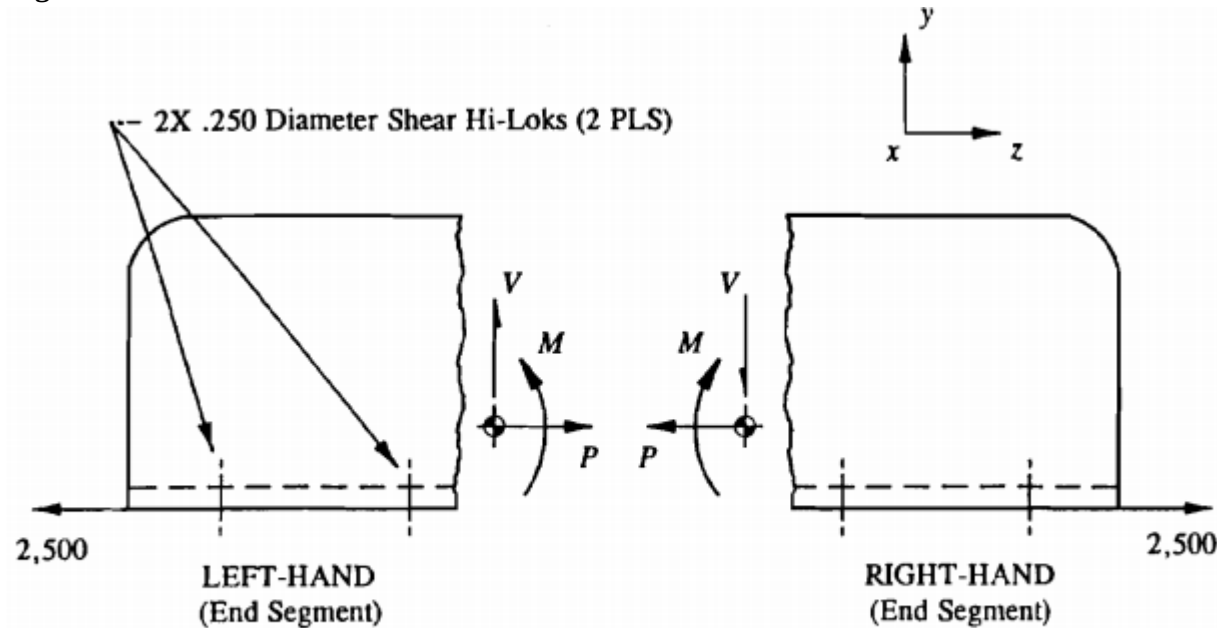


FIGURE 2-58 System of internal forces shown on exposed sections of the beam.

Solution – cont'd:

From this result, and considering the homogeneous construction of this beam, it is evident that the internal loads V , P , and M are constant values along the entire beam. To verify this generalization, the same internal loads analysis can be performed, but this time, at several other sections along the beam structure. Looking ahead to Fig. 2-60, it can be seen that this moment will act in a plane indicated by the moment vector M . Also shown in that same figure are the equivalent component moments M_{xp} and M_{yp} which must appropriately act around the principal bending axes x_p and y_p of the cross-sectional area, respectively. Clearly, the application of the equations of static equilibrium has demonstrated how an eccentrically applied tension force can effectively be carried (across any section) by the structural member itself. Before the magnitude of this moment can be evaluated, however, the eccentricity e must first be found. To accomplish this, the tabulation method of Appendix F is employed using the unshaded areas of Section A-A.

Solution – cont'd:

The element areas assigned for this section are shown in Fig. 2-59. The actual computations are performed in below:

Moment of Inertia I_x around the \bar{x} -axis

Element	b	h	y	A	Ay	Ay^2	I_o
1	0.160	1.350	0.825	0.216	0.178	0.147	0.033
2	0.675	0.150	0.075	0.101	0.008	0.001	0.000
3	0.250	0.150	0.075	-0.037	-0.003	-0.000	-0.000
4	0.375	0.150	0.075	0.056	0.004	0.000	0.000
Total				0.336	0.187	0.148	0.033

$$Y_{cg} = \frac{\sum Ay}{\sum A} = \frac{.187}{.336} = .557 \text{ in}$$

$$I_x = I_{cg} = \sum I_o + \sum Ay^2 - Y_{cg}(\sum Ay)$$

$$I_x = .033 + .148 - .557(.187) = .077 \text{ in}^4.$$

Moment of Inertia I_y around the \bar{y} -axis

Element	b	h	x	A	Ax	Ax^2	I_o
1	1.350	0.160	0.080	0.216	0.017	0.001	0.000
2	0.150	0.675	0.337	0.101	0.034	0.011	0.004
3	0.150	0.250	0.800	-0.037	-0.030	-0.024	-0.000
4	0.150	0.375	1.112	0.056	0.063	0.070	0.001
Total				0.336	0.084	0.058	0.005

$$X_{cg} = \frac{\sum Ax}{\sum A} = \frac{.084}{.336} = .250 \text{ in}$$

$$I_y = I_{cg} = \sum I_o + \sum Ax^2 - X_{cg}(\sum Ax)$$

$$I_y = .005 + .058 - .250(.084) = .042 \text{ in}^4.$$

Solution – cont'd:

Now, having located the centroid of this section area, the eccentricity e of the applied tension force can be determined. The numerical details of this computation, however, are left as an exercise for the engineer to complete. The predetermined value of e is .783 in. With this value, the magnitude of the internal bending moment M may also be computed. This gives:

$$M = 2500(e) = 2500(0.783) = 1957 \text{ in-lb}$$

This moment is now resolved into two equivalent components M_{x_p} and M_{y_p} which act in planes containing the principal bending axes x_p and y_p respectively:

$$M_{x_p} = M \cos \beta$$

$$M_{y_p} = M \sin \beta$$

Solution – cont'd:

This corresponds to Fig. 2-60. The proper orientation of the principal bending axes and their corresponding principal moments of inertia are computed using Eqs. A-10 through A-13 of Appendix G as follows:

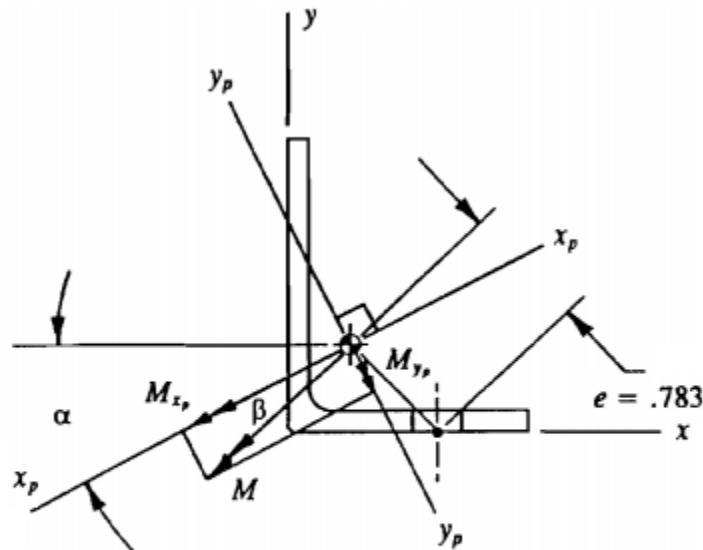


FIGURE 2-60 The moment M resolved into equivalent component moments acting in planes containing the principal bending axes.

$$\begin{aligned}
 (1) \quad I_{xy} &= \sum Axy - AX_{cg}Y_{cg} \\
 &= .216(.080)(.825) + .101(.337)(.075) - .037(.800)(.075) \\
 &\quad + .056(1.112)(.075) - .336(.250)(.557) \\
 &= .014 + .003 - .002 + .005 - .047 \\
 I_{xy} &= -.027 \text{ in}^4.
 \end{aligned}$$

$$\begin{aligned}
 (2) \quad \tan 2\alpha &= \frac{2I_{xy}}{I_y - I_x} = \frac{2(-.027)}{.042 - .077} = 1.543 \\
 2\alpha &= \tan^{-1} 1.543 = 57.1^\circ \\
 \alpha &= 28.5^\circ.
 \end{aligned}$$

$$\begin{aligned}
 (3) \quad I_{x_p} &= I_x \cos^2 \alpha + I_y \sin^2 \alpha - I_{xy} \sin 2\alpha \\
 &= .077(.879)^2 + .042(.477)^2 - (-.027)(.839) \\
 &= .059 + .010 + .023 \\
 I_{x_p} &= .092 \text{ in}^4 \quad (\text{maximum principal moment of inertia}).
 \end{aligned}$$

$$\begin{aligned}
 (4) \quad I_{y_p} &= I_x \sin^2 \alpha + I_y \cos^2 \alpha + I_{xy} \sin 2\alpha \\
 &= .077(.477)^2 + .042(.879)^2 + (-.027)(.839) \\
 &= .018 + .032 - .023 \\
 I_{y_p} &= .027 \text{ in}^4 \quad (\text{minimum principal moment of inertia}).
 \end{aligned}$$

Solution – cont'd:

With the basic dimensions of this cross-sectional area properly described, and the value of α known, the angle β found to be 16.1° . The actual proof of this is left for the engineer's own verification. Substituting the angle β into the two expressions for component moments gives:

$$M_{x_p} = M \cos \beta = 1957 \cos 16.1^\circ = 1880 \text{ in-lb}$$

$$M_{y_p} = M \sin \beta = 1957 \sin 16.1^\circ = 543 \text{ in-lb.}$$

The remaining solution is essentially divided into two separate bending solutions using the component moments around each of their respective principal bending axes of the cross-sectional area. According to Eq. 2-21, the computed stresses of each solution are then superimposed together with the corresponding axial stresses.

Solution – cont'd:

For easy reference, this equation is rewritten as follows:

$$f = \pm \frac{P}{A} \pm \frac{M_{x_p} c_{y_p}}{I_{x_p}} \pm \frac{M_{y_p} c_{x_p}}{I_{y_p}}$$

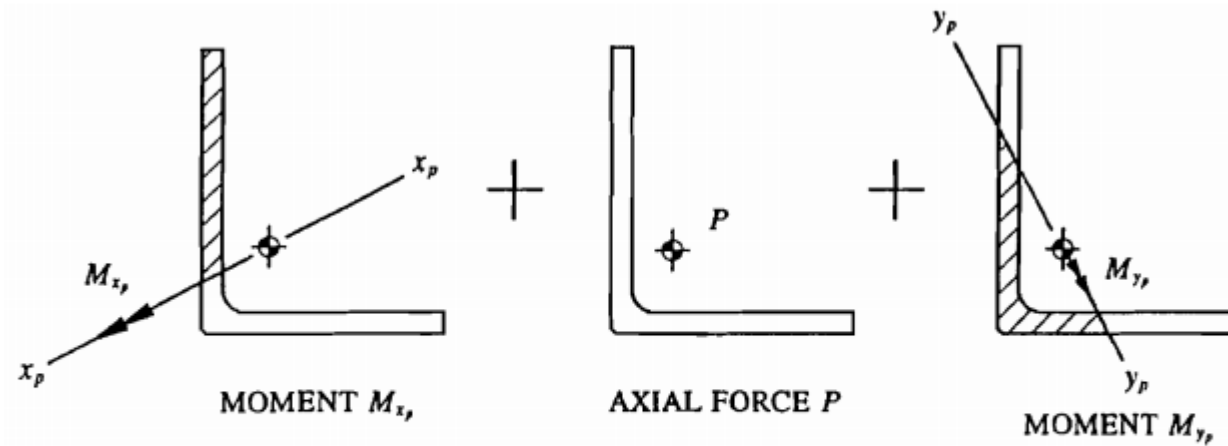


FIGURE 2-61 Diagram shows stresses that are produced on the surface of a cross-sectional area for different loading types. Compression stresses are shown cross-hatched, while areas in tension are not.